

Consensus Docking and ADMET Profiling of Pomegranate Leaf Phytochemicals as Potential Dual Inhibitors of *Candida albicans* Virulence and Ergosterol Biosynthesis

Shukurana Sulaiman Adam

 <https://orcid.org/0009-0007-0441-3223>

Department of Human Anatomy, Faculty of Basic Medical Sciences, Federal University Dutse, Jigawa State, Nigeria

 <https://ror.org/0278jft56>

Corresponding author: shukurana.sulaiman.adam@gmail.com

Received 2026-04-04

Accepted 2026-05-15

Published 2026-06-29

How to Cite: Adam SS. Consensus Docking and ADMET Profiling of Pomegranate Leaf Phytochemicals as Potential Dual Inhibitors of *Candida albicans* Virulence and Ergosterol Biosynthesis. Journal of Medical Science. 2026 June;95(2);e1594. doi:10.20883/medical.e1594

 <https://doi.org/10.20883/medical.e1594>

Keywords: antifungal agents, *Candida albicans*, ellagic acid, molecular docking, quercetin



© 2026 by the Author(s). This is an open access article distributed under the terms and conditions of the Creative Commons Attribution (CC BY-NC) licence. Published by Poznan University of Medical Sciences

ABSTRACT

Background. The increasing resistance of *Candida albicans* to conventional azole therapies necessitates the discovery of novel antifungal agents that target both metabolic pathways and virulence factors. This in silico study investigated the potential of pomegranate leaf phytochemicals as dual inhibitors of lanosterol 14 α -demethylase (CYP51), essential for ergosterol biosynthesis, and secreted aspartic protease 2 (SAP2), a mediator of fungal virulence.

Material and methods. A consensus docking approach was employed using three independent engines: AutoDock Vina, AutoDock4, and LeDock. Seven phytochemicals were screened against crystal structures of CYP51 and SAP2. Reliability was validated by redocking, and binding interactions were analysed using 3D and 2D visualisations in Discovery Studio Visualizer (2025). The pharmacokinetics, drug-likeness, and toxicity of the compounds were assessed using the SwissADME and pkCSM tools.

Results. Consensus Z-scores identified two distinct classes of inhibitors. Quercetin was predicted as the primary consensus lead against CYP51 (Z-score: -0.98), outperforming fluconazole (Z-score: 0.77) by targeting residues in the substrate-access channel (Ser378, Leu87) rather than traditional heme coordination. Ellagic acid was the primary consensus lead for SAP2, predicted to act as a molecular wedge that may restrict mobility of the enzyme's flexible flap region (Tyr84). Luteolin and apigenin, identified as secondary lead candidates, exhibited consistent binding across both targets. All prioritised compounds demonstrated favourable ADMET profiles, adhering to Lipinski's Rule of Five with high gastrointestinal absorption.

Conclusions. The findings suggest a specialist-generalist dichotomy among pomegranate phytochemicals. While quercetin and ellagic acid suggest high-potency targeted inhibition, the dual-target engagement of luteolin and apigenin may offer a predicted strategic advantage in reducing the evolutionary probability of resistance. These results provide a molecular framework for the development of plant-derived multi-target antifungal therapies.

Introduction

The growing azole resistance crisis reflects the need to identify alternative or complementary

antifungals that target both classical and non-classical virulence mechanisms. In recent years, natural products have gained renewed attention as valuable sources of diverse bioactive com-

pounds with antimicrobial efficacy. Plant-derived polyphenols, particularly flavonoids, have demonstrated broad antifungal activity through multiple mechanisms, including membrane disruption, enzyme inhibition, oxidative stress induction, and modulation of virulence factors [1]. The structural complexity and multi-target potential of these compounds make them promising candidates in the search for novel antifungal leads.

Punica granatum L. (pomegranate), a species with a long history of traditional medicinal use, is abundant in polyphenols, flavonoids, and tannins, which have been associated with antimicrobial and antioxidant activities [2,3]. Previous investigations have demonstrated the antifungal activity of pomegranate extracts, particularly peel phenolics such as punicalagin and punicalin, against pathogenic fungi [4]; however, most studies have focused on fruit peel-derived phenolics. In contrast, the phytochemical composition and target-specific antifungal potential of leaf-derived constituents of pomegranate leaves remain comparatively underexplored. Although there is growing recognition that other plant parts, such as leaves, may harbour unique bioactive compounds that could interfere with essential fungal targets or modulate virulence pathways [2], systematic, target-based investigations of pomegranate leaf phytochemicals are currently lacking. While pomegranate peel is a well-documented source of hydrolysable tannins, the leaf metabolome offers a different profile characterised by a higher density of specific flavonoids. Previous HPLC, FAB-mass spectrometry, and NMR phytochemical profiling studies have confirmed the presence of flavonoids and related polyphenols in hydroethanolic *P. granatum* leaf extracts [5-8]. Quantitative analyses reported ellagic acid concentrations ranging from approximately 1.30 to 6.46 mg/g dry weight, depending on seasonal and extraction conditions. At the same time, total flavonoid yields in leaf extracts reached up to 147.4 mg/g dry weight [9,10]. Quercetin and related flavonoids have also been identified as significant bioactive constituents of the leaf metabolome [7,11].

In silico approaches have become indispensable tools in early-stage drug discovery [12], enabling efficient screening of candidate compounds, elucidation of molecular interactions, and prediction of absorption, distribution, metabolism, excretion, and toxicity (ADMET) properties.

These computational approaches offer insights into ligand–protein binding affinities and interaction geometries, thereby guiding the identification of promising lead compounds before experimental validation. While molecular docking has become a cornerstone of virtual screening, traditional workflows often rely on a single docking engine. Such single-engine approaches are frequently limited by scoring bias, in which the mathematical algorithm may overpredict the affinity of certain chemical classes while producing false positives for others. By combining multiple independent docking algorithms, each with different scoring functions, consensus methods can cancel out individual software errors, providing a more robust and validated ranking of potential leads. To date, no molecular docking studies have systematically evaluated major leaf-derived phytoconstituents of *P. granatum* against validated antifungal targets, such as lanosterol 14 α -demethylase (CYP51) and secreted aspartic proteinase 2 (SAP2) of *C. albicans*.

Given the increasing resistance to conventional antifungal agents and the limited structural characterisation of pomegranate leaf phytochemicals in an antifungal context, a focused computational investigation is warranted. Therefore, the present study aimed to evaluate major bioactive constituents identified from *P. granatum* systematically leaves for their predicted inhibitory potential against CYP51 and SAP2 using consensus molecular docking, binding interaction analysis, and ADMET profiling, to identify promising multi-target antifungal lead candidates for future experimental validation.

Materials and methods

Protein selection and preparation

Two *Candida albicans* proteins: (CYP51, PDB ID: 5V5Z and SAP2, PDB ID: 1EAG) were selected. High-resolution crystal structures (< 3.0 Å) were downloaded from the Protein Data Bank (PDB; <https://www.rcsb.org>). Protein preparation was performed using AMDock v1.4.x [13], which internally uses routines from AutoDock Tools v.1.5.7 [14] to prepare receptor structures. This automated procedure included the removal of co-crystallised ligands and water molecules, the addition of polar hydrogens, the merging of non-polar hydro-

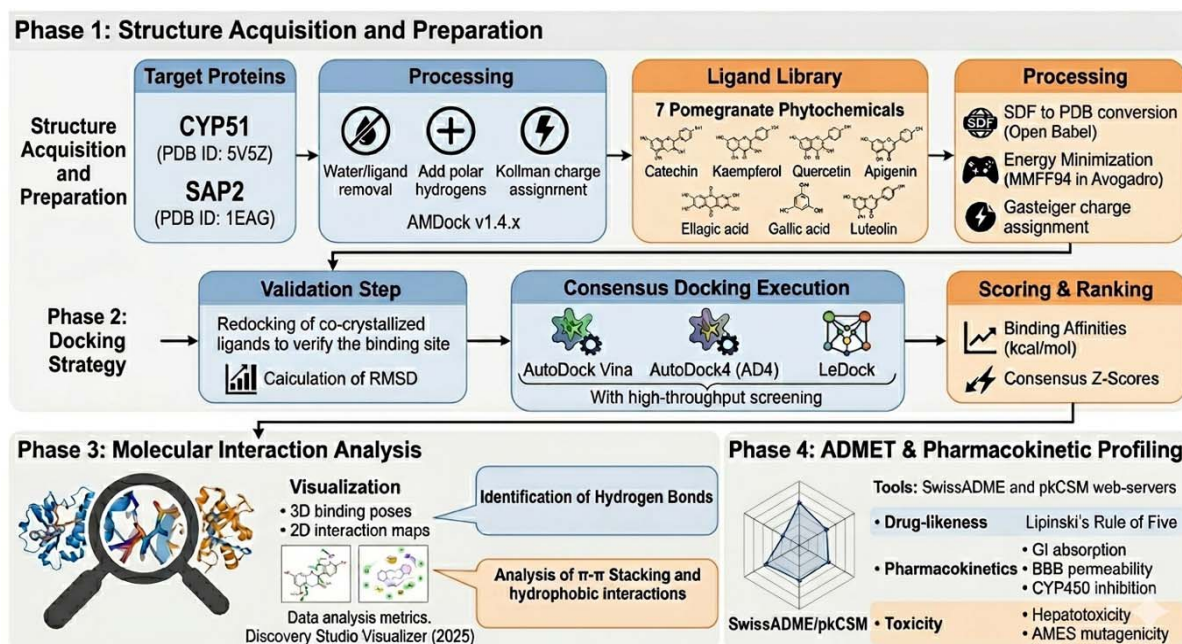


Figure 1. Workflow of the in silico molecular docking study.

gens, the assignment of Kollman charges, and the conversion of the structures into PDBQT format suitable for docking.

Ligand selection and preparation

Compounds were selected based on published phytochemical profiling studies. These include catechin, kaempferol, quercetin, and apigenin [15], ellagic acid [16], gallic acid [17], and luteolin [18]. Three-dimensional structures of the selected phytochemicals were obtained from PubChem (<https://pubchem.ncbi.nlm.nih.gov>) in SDF format. The structures were converted to PDB format using Open Babel v2.4.1 [19] and subsequently energy-minimised using the MMFF94 force field in Avogadro [20] to obtain stable conformations. Ligands were prepared for docking using AMDDock v1.4.x [13] which automatically assigns Gasteiger charges, detects rotatable bonds, adds hydrogens, and converts the ligands to PDBQT format compatible with the docking engine. Fluconazole and Pepstatin A were included as reference ligands for CYP51 and SAP2, respectively, and prepared using the same procedure.

Redocking validation and visualisation

To validate the docking protocol, the co-crystallised ligands were re-docked into their respective binding sites. Redocking validation was per-

formed using the online web server LigRMSD [21], which compared the predicted poses with the experimental crystallographic conformations. The redocked poses showed high geometric similarity to the native ligands, yielding root-mean-square deviation (RMSD) values of 0.34 Å for CYP51 and 0.73 Å for SAP2, confirming the reliability of the docking parameters. The superimposition of the native and redocked ligands is shown in **Supplementary files 1 and 2**.

Consensus docking

Consensus docking was performed using three docking platforms to evaluate the robustness of binding predictions. The study employs a tri-engine consensus docking workflow to calculate a consensus Z-score to eliminate algorithmic bias. Docking simulations were performed on a laptop running Windows 11 (64-bit) equipped with an Intel® Core™ i7-10510U processor and 16 GB RAM. Molecular docking was carried out using the following docking engines:

AMDDock v1.4.x [13]: For the CYP51 protein target, the search space was defined using a grid box of 39.0 Å × 39.0 Å × 39.0 Å centered at coordinates (X: -44.8, Y: -10.7, Z: 22.3) and grid box of 27.0 Å × 27.0 Å × 27.0 Å centered at coordinates (X: 41.97, Y: 22.59, Z: 11.47 for SAP2) with an exhaustiveness value of 8. Each ligand was docked inde-

pendently against each protein target, and the best binding pose was selected based on the lowest binding affinity (kcal/mol).

LeDock [22]: Ligand and protein files were prepared in accordance with LeDock requirements. The protein structure was first prepared using the LePro program, which automatically added hydrogen atoms, assigned CHARMM force field charges, and removed water molecules and cofactors. Ligands were prepared in SYBYL Mol2 format, and energy minimisation was performed to ensure an optimal starting 3D conformation. The docking parameters were defined in a configuration file (dock.in), with the search space and coordinates similar to those of AutoDock Vina and AutoDock4. For each ligand, 20 docking runs were executed with an RMSD clustering tolerance of 1.0 Å. Top-ranked poses were selected based on predicted binding energy and orientation.

Binding affinities and interaction features were tabulated. Consensus Z-scores were calculated by averaging the standardised Z-scores from the three docking platforms for each ligand using the formula:

$$Z = \frac{x - \mu}{\sigma}$$

(where x is the score, μ is the mean, and σ is the standard deviation). Docked complexes were visualised and analysed using Discovery Studio Visualizer 2025 [23]. Interactions such as hydrogen bonding, hydrophobic contacts, and π - π interactions were examined using two-dimensional interaction diagrams. Key interacting residues were compared with previously reported active site residues for each protein.

ADMET and drug-likeness prediction

Pharmacokinetic and toxicity profiles were evaluated using the web-based tools SwissADME [24] and pkCSM [25]. Parameters analysed included Lipinski's Rule of Five compliance, gastrointestinal absorption, blood-brain barrier permeability, and cytochrome P450 inhibition. These data were used to assess drug-likeness, pharmacokinetic suitability, and potential drug-drug interaction risks, and to prioritise ligands for further study.

Results

Binding affinity against CYP51 and SAP2

Among all tested compounds, quercetin exhibited the strongest binding affinity across all docking engines toward CYP51 (see **Table 1**), outperforming the reference antifungal drug fluconazole. At the same time, ellagic acid exhibited the strongest binding affinity towards SAP2 (see **Table 2**). Luteolin and apigenin also demonstrated notable affinities, ranking second and third, respectively, towards both CYP51 and SAP2. In contrast, gallic acid exhibited weaker binding energies across all docking engines.

Binding interaction and residue analysis of CYP51

The docked complex reveals that quercetin is stably accommodated within the enzyme's catalytic pocket, forming multiple non-covalent interactions with functionally relevant amino acid residues. Quercetin, as a primary lead, forms hydrogen-bond interactions with the Ser378 residue located in proximity to the catalytic region of

Table 1. Consensus docking scores of *P. granatum* leaf compounds against CYP51.

| Compound | PubChem CID | Vina score (kcal/mol) | AD4 score (kcal/mol) | LeDock score (kcal/mol) | Consensus Z-score | Ranking |
|--------------|-------------|-----------------------|----------------------|-------------------------|-------------------|---------|
| Apigenin | 5280443 | -8.7 | -7.90 | -4.74 | -0.50 | 3 |
| Catechin | 9064 | -8.8 | -7.16 | -4.92 | -0.43 | 4 |
| Ellagic acid | 5281855 | -7.9 | -7.66 | -4.71 | -0.13 | 6 |
| Gallic acid | 370 | -5.9 | -5.18 | -3.72 | 1.97 | 8 |
| Kaempferol | 5280863 | -8.7 | -7.05 | -4.61 | -0.15 | 5 |
| Luteolin | 5280445 | -8.6 | -7.94 | -4.85 | -0.55 | 2 |
| Quercetin | 5280343 | -8.7 | -7.93 | -5.44 | -0.98 | 1 |
| Fluconazole | 3365 | -7.8 | -5.55 | -4.37 | 0.77 | 7 |

Note: The consensus Z-score represents the mean standardised docking performance across the three docking platforms. A Z-score of 0 represents the average docking performance of all screened compounds, negative values indicate stronger-than-average predicted consensus binding affinity, and positive values indicate weaker-than-average predicted binding performance.

CYP51 (see **Figure 2A**). These hydrogen bonds contribute to the stabilisation of the ligand within the active site and indicate a favourable orientation of quercetin hydroxyl groups toward polar residues. The π - π stacking interactions with Phe233 and Ser453 suggest a potential channel-occlusion mechanism that, if sustained, could interfere with catalytic activity. Similarly, apigenin and luteolin, as secondary lead candidates, formed hydrogen bonds with key residues such as Ser378, Tyr460, and Gly466, and engaged in π - π interactions with aromatic residues including His377, Phe228, and Phe233 (see **Table 3**). These interactions are critical for maintaining ligand stability within the heme-binding pocket and may contribute to inhibition of sterol biosynthesis. In contrast, gallic acid displayed limited interaction with CYP51, forming no significant hydrogen bonds and only weak π - π interactions with Phe463, which may account for its poor docking performance.

Binding interaction and residue analysis of SAP2

For SAP2, ellagic acid, the top-ranked primary consensus lead, demonstrated strong binding through hydrogen bond interactions with catalytic residues Asp86 and Ser88, as well as π - π stacking with Tyr84, a key residue within the flap region (see **Figure 2C**). These interactions suggest potential anchoring within the active site and possible restriction of the enzyme's flexible regions. Luteolin and apigenin also showed favourable binding patterns, forming hydrogen bonds with Asp120 and π - π interactions with Tyr84, indicating consistent engagement with critical residues involved in protease activity. This suggests that secondary compounds, such as ellagic acid, may contribute to restricting flap-region mobility of SAP2. Gallic acid, as a comparative candidate, however, exhibited hydrogen-bond interactions with Asp86 and Gly83, with no π - π stacking, which possibly explains its lower binding affinity observed with SAP2 (see **Table 3**).

Table 2. Consensus docking scores of *P. granatum* leaf compounds against SAP2.

| Compound | PubChem CID | Vina Score (kcal/mol) | AD4 Score (kcal/mol) | LeDock Score (kcal/mol) | Consensus Z-score | Ranking |
|--------------|-------------|-----------------------|----------------------|-------------------------|-------------------|---------|
| Apigenin | 5280443 | -7.6 | -6.59 | -4.32 | -0.26 | 3 |
| Catechin | 9064 | -7.4 | -6.11 | -4.12 | 0.06 | 6 |
| Ellagic acid | 5281855 | -7.7 | -5.79 | -5.26 | -0.64 | 1 |
| Gallic acid | 370 | -5.2 | -3.89 | -3.53 | 1.84 | 8 |
| Kaempferol | 5280863 | -7.6 | -6.00 | -4.50 | -0.21 | 4 |
| Luteolin | 5280445 | -7.7 | -6.26 | -4.49 | -0.31 | 2 |
| Quercetin | 5280343 | -7.7 | -6.24 | -4.85 | -0.52 | 7 |
| Pepstatin A | 5478883 | -7.8 | -3.21 | -5.20 | 0.05 | 5 |

Note: The consensus Z-score represents the mean standardised docking performance across the three docking platforms. A Z-score of 0 represents the average docking performance of all screened compounds, negative values indicate stronger-than-average predicted consensus binding affinity, and positive values indicate weaker-than-average predicted binding performance.

Table 3. Residue interactions of primary, secondary, positive, and negative controls with CYP51 and SAP2.

| Protein | Compound | Amino acid residues involved | |
|---------|--------------|------------------------------|--------------------------------|
| | | H-bond | Pi-stacked |
| CYP51 | Quercetin | Ser378 | Phe233 |
| | Apigenin | Ser378, Tyr460, Gly466 | His377 |
| | Luteolin | Ser378, His377 | His377, Phe228, Tyr118, Phe233 |
| | Fluconazole | Ile471 | His468, Phe463 |
| | Gallic acid | – | Phe463 |
| SAP2 | Ellagic acid | Asp86, Ser88 | Tyr84 |
| | Apigenin | Asp120 | Tyr84 |
| | Luteolin | Asp120 | Tyr84 |
| | Pepstatin A | – | – |
| | Gallic acid | Asp86, Gly83 | – |

Only high affinity hydrogen bonds with interatomic distances < 3.5 Å are listed. Standard hydrophobic interactions (<5.0 Å) providing auxiliary stability are discussed in text. Quercetin and ellagic acid = primary leads; apigenin and luteolin = secondary leads; fluconazole and pepstatin A = positive control; Gallic acid = negative control.

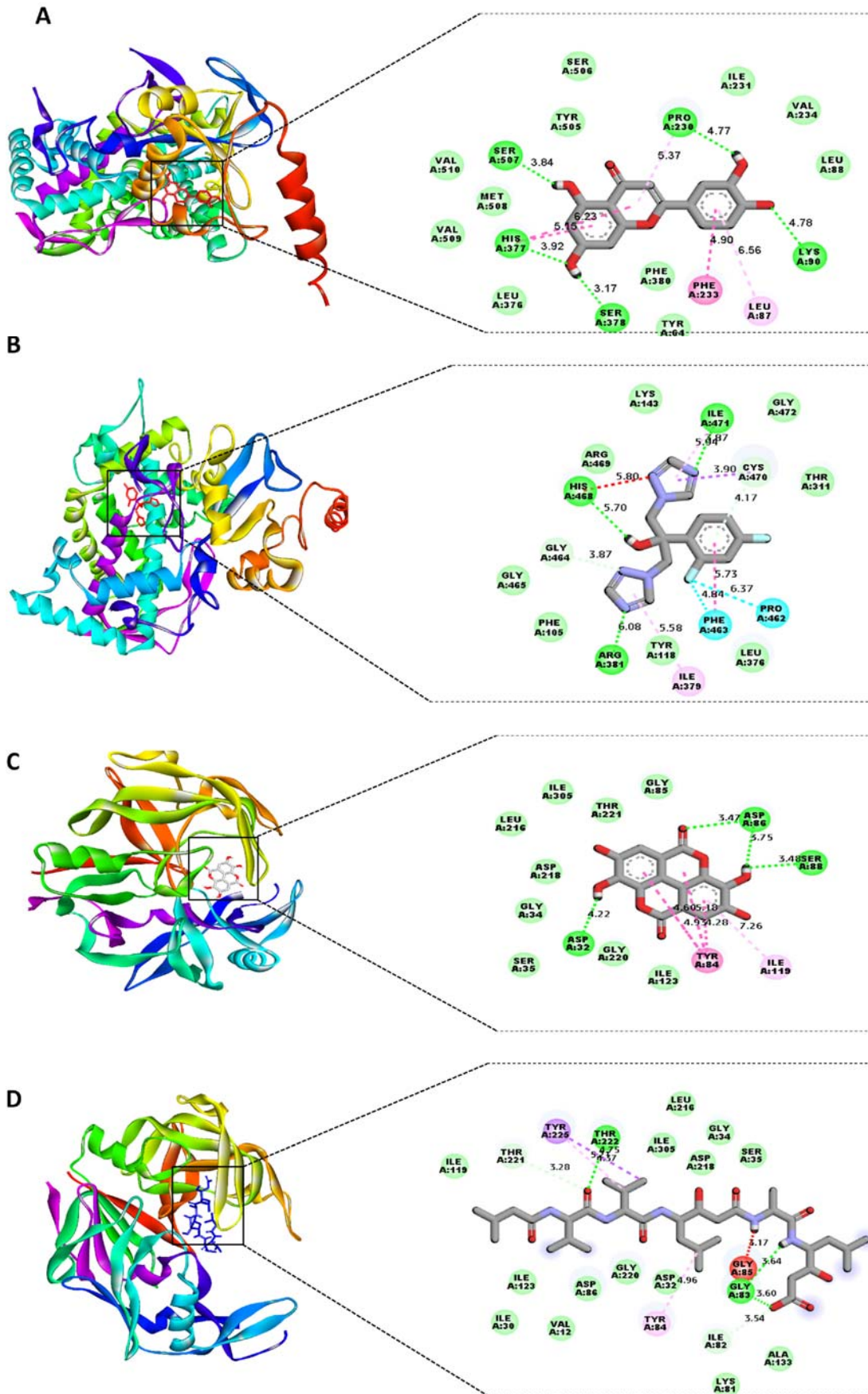


Figure 2. 3D/2D interactions of (A) Quercetin and (B) Fluconazole with CYP51. Figure (C) shows Ellagic acid and (D) Pepstatin A with SAP2. Hydrogen bonds are shown in green dashed lines, hydrophobic contacts in purple/magenta.

Physicochemical properties and drug-likeness

Table 4 shows that both the primary (quercetin and ellagic acid) and secondary (luteolin and apigenin) lead compounds exhibit higher drug-likeness profiles compared to the peptide-based inhibitor, pepstatin A. All identified leads strictly adhered to Lipinski's Rule of Five (MW < 500 Da, HBD < 5, HBA < 10, and Log P < 5). Conversely, pepstatin A exhibited significant violations (MW: 685.89, HBD: 8), suggesting suboptimal oral bioavailability. Furthermore, the compounds demonstrated low molecular complexity, with rotatable bond counts between 0 and 1, and moderate Topological Polar Surface Area (TPSA) values (90.90–131.36 Å²), all below the critical 140 Å² threshold, which are indicative of favourable oral bioavailability.

All prioritised primary and secondary lead compounds demonstrated high gastrointestinal (GI) absorption, comparable to the clinical standard, fluconazole. Additionally, unlike the reference compounds, the leads were not identified as substrates for P-glycoprotein (P-gp), suggesting a reduced risk of efflux-mediated drug resistance.

Metabolic profiling indicated that quercetin, luteolin, and apigenin may inhibit the cytochrome P450 enzymes CYP3A4 and CYP2D6. In contrast, ellagic acid exhibited no such inhibition, presenting a more favourable metabolic profile. Furthermore, synthetic accessibility scores (2.96–3.23) categorise these natural compounds as highly feasible to synthesise or isolate. All compounds, except apigenin, triggered one PAINS alert.

Comparative pharmacokinetic and toxicity analysis

ADMET profiling further confirmed that the primary consensus lead (quercetin) and secondary candidates (apigenin and luteolin) exhibit potentially enhanced safety and absorption profiles relative to conventional antifungal agents (see **Table 5**). Quantitative in silico predictions of Human Intestinal Absorption (HIA) revealed high absorption percentages, especially for ellagic acid (86.68%) and for the secondary lead, apigenin (93.25%). These values represent a marked improvement over the protease inhibitor pepstatin A, which demonstrated negligible absorption (4.33%). Furthermore, Caco-2 permeability

Table 4. In silico drug-likeness, absorption and physicochemical properties of selected compounds.

| Parameter | Quercetin | Ellagic acid | Luteolin | Apigenin | Fluconazole | Pepstatin A |
|---------------------------------------|-----------|--------------|----------|----------|--------------|-------------|
| Physicochemistry | | | | | | |
| MW (g/mol) | 302.24 | 302.19 | 286.24 | 270.24 | 306.27 | 685.89 |
| TPSA (Å ²) | 131.36 | 141.34 | 111.13 | 90.90 | 81.65 | 223.26 |
| HBD | 5 | 4 | 4 | 3 | 1 | 8 |
| HBA | 7 | 8 | 6 | 5 | 7 | 9 |
| Rotatable bonds | 1 | 0 | 1 | 1 | 5 | 27 |
| Lipophilicity | | | | | | |
| Consensus Log <i>P</i> _{o/w} | 1.23 | 1.00 | 1.73 | 2.11 | 0.88 | 2.37 |
| Log <i>P</i> _{o/w} (XLOGP3) | 1.54 | 1.10 | 2.53 | 3.02 | 0.35 | 2.99 |
| Solubility class | Soluble | Soluble | Moderate | Moderate | Very soluble | Poorly |
| Pharmacokinetics | | | | | | |
| GI absorption | High | High | High | High | High | Low |
| BBB permeant | No | No | No | No | No | No |
| P-gp substrate | No | No | No | No | Yes | Yes |
| CYP inhibitor: | | | | | | |
| – CYP3A4 | Yes | No | Yes | Yes | No | No |
| – CYP2D6 | Yes | No | Yes | Yes | No | No |
| – CYP2C9 | No | No | No | No | No | No |
| Lipinski | Yes | Yes | Yes | Yes | Yes | No |
| Bioavailability score | 0.55 | 0.55 | 0.55 | 0.55 | 0.55 | 0.11 |
| PAINS (alerts) | 1 | 1 | 1 | 0 | 0 | 0 |
| Synthetic accessibility | 3.23 | 3.17 | 3.02 | 2.96 | 2.45 | 6.65 |

MW = Molecular weight; TPSA = Topological polar surface area; HBD = Hydrogen bond donor; HBA = Hydrogen bond acceptor; Log *P* = Lipophilicity; GI = Gastrointestinal; BBB = Blood brain barrier; PAINS = Pan-assay interferences compounds

Table 5. Comparative pharmacokinetic and toxicity profiles of compounds.

| Compound | PubChem CID | Water solubility (log mol/L) | Caco-2 (log P _{app}) | HIA (%) | Skin (log Kp) Permeability | VD _{ss} (log L/kg) | BBB (log BB) Permeant | AMES toxicity | Hepatotoxicity |
|--------------|-------------|------------------------------|--------------------------------|---------|----------------------------|-----------------------------|-----------------------|---------------|----------------|
| Apigenin | 5280443 | -3.32 | 1.00 | 93.25 | -2.73 | 0.82 | -0.73 | No | No |
| Catechin | 9064 | -3.11 | -0.28 | 68.82 | -2.73 | 1.02 | -1.05 | No | No |
| Ellagic acid | 5281855 | -3.18 | 0.33 | 86.68 | -2.73 | 0.37 | -1.27 | No | No |
| Gallic acid | 370 | -2.56 | -0.08 | 43.37 | -2.73 | -1.85 | -1.10 | No | No |
| Kaempferol | 5280863 | -3.04 | 0.03 | 74.29 | -2.73 | 1.27 | -0.93 | No | No |
| Luteolin | 5280445 | -3.09 | 0.09 | 81.13 | -2.73 | 1.15 | -0.90 | No | No |
| Quercetin | 5280343 | -2.92 | -0.22 | 77.20 | -2.73 | 1.55 | -1.09 | No | No |
| Fluconazole | 3365 | -3.02 | -0.38 | 85.47 | -3.29 | -1.32 | -1.07 | Yes | Yes |
| Pepstatin A | 5478883 | -3.06 | -0.20 | 4.33 | -2.73 | -1.70 | -1.31 | No | Yes |

HIA = Human intestinal absorption; VD_{ss} = Volume of distribution at steady state; BBB = Blood brain barrier.

assays identified apigenin as a highly permeable candidate (log P_{app} = 1.00), while fluconazole and quercetin exhibited more moderate permeability coefficients of -0.38 and -0.22, respectively. The steady-state volume of distribution (VD_{ss}) and blood-brain barrier (BBB) metrics indicate that quercetin had a significantly higher VD_{ss} (1.55 log L/kg) than fluconazole (-1.32 log L/kg), suggesting more extensive distribution into peripheral tissues. Regarding safety, all primary and secondary leads were classified as non-permeant to the BBB, with log BB values ranging from -0.73 to -1.27.

Evaluation of mutagenic potential using the AMES test revealed that all lead compounds were non-mutagenic (AMES-negative). In contrast, the clinical standard, fluconazole, yielded a positive AMES result, suggesting a potential risk of genetic toxicity. Furthermore, organ toxicity predictions indicated that all lead phytochemicals were non-hepatotoxic. This stands in marked contrast to both fluconazole and pepstatin A, which were flagged for potential hepatotoxicity.

Discussion

This study employs a consensus docking workflow to evaluate selected pomegranate leaf phytochemicals against *Candida albicans* targets: lanosterol 14 α -demethylase (CYP51) and secreted aspartic protease 2 (SAP2). Based on reproducible tri-engine consensus Z-scores, quercetin and ellagic acid are designated as primary consensus leads due to their target-preferential bind-

ing. Luteolin and apigenin, while demonstrating consistent cross-target affinity across all docking platforms, are discussed as secondary candidates. The ADMET and dual-target characteristics of the secondary leads are interpreted as comparative candidates.

Quercetin consistently ranked as the top primary consensus lead for CYP51 across all three docking engines (consensus Z-score = -0.98), surpassing the reference antifungal fluconazole (consensus Z-score = 0.77). Hydrogen bonds mediate its binding to Ser378, π - π interactions with Phe233, and stabilisation by Ser453, Gly466, and Tyr460 within the C-terminal loop, which is part of the heme-binding region in many CYP51 structures. This orientation is predicted to occlude the substrate access channel, suggesting a potential mechanism of competitive inhibition of lanosterol entry and subsequent suppression of ergosterol biosynthesis—a hypothesis that requires MD simulation and experimental assay to confirm, which is mechanistically distinct from heme-iron coordination typically observed with azoles. While prior studies [26,27] focused primarily onazole coordination with heme iron, the present findings indicate that quercetin preferentially targets residues lining the substrate access channel, providing a potential mechanism to bypass resistance arising from alterations in heme coordination. Experimental studies confirm that quercetin inhibits biofilm formation, reduces adherence and hyphal transition, and downregulates virulence-associated genes (ALS1, ALS3, HWP1) in both planktonic and biofilm models [28]. Furthermore, when combined with flucon-

azole, quercetin synergistically inhibits biofilms in fluconazole-resistant *C. albicans* isolates and reduces the pathogenic burden in murine vulvovaginal candidiasis models [29]. These experimental results highlight that quercetin's antifungal potential extends beyond predicted binding energies, suggesting broader modulation of cell-surface properties, virulence mechanisms, and biofilm dynamics [30].

Ellagic acid was identified as the top primary consensus lead for SAP2 (consensus Z-score = -0.64), surpassing Pepstatin A (consensus Z-score = 0.05) across all consensus docking engines. Key interactions involve catalytic residues Asp86 and Ser88 and engagement of the flexible flap region via π - π stacking with Tyr84. The mobility of the flap region is critical for substrate binding and catalytic turnover, and Tyr84 has been identified as essential for flap closure and catalytic efficiency [31]. Ellagic acid is predicted to act as a molecular wedge that may restrict flap mobility, potentially favouring an inactive-like conformation of SAP2—though whether this predicted restriction translates to sustained inhibition under dynamic physiological conditions requires MD simulations to confirm. This aligns with prior studies suggesting that targeted immobilisation of flap residues can effectively suppress protease activity [32,33]. While inhibitors targeting SAP2's flap region are uncommon, this mode of interaction suggests that flavonoids can act beyond simple active-site competition, disrupting enzyme flexibility and substrate processing. These structural insights complement functional studies showing that ellagic acid suppresses hyphal transition and HWP1 expression [34], providing a mechanistic explanation linking phenotypic inhibition to direct molecular interactions within the SAP2 active site. Physiologically, ellagic acid exhibits broad antifungal activity against *Candida* species and other fungi, including inhibition of ergosterol biosynthesis and disruption of membrane integrity. In certain cases, its antifungal potency matches that of fluconazole, and it has been reported to reduce CYP51 enzymatic activity in model systems, reflecting multifaceted effects on fungal physiology [35,36].

In contrast to the target-preferential behaviour of quercetin and ellagic acid, the secondary comparative lead candidates, luteolin and api-

genin, consistently exhibited dual-target behaviour across CYP51 and SAP2 and showed reproducible binding across all three docking engines. This stability suggests genuine multi-target potential rather than algorithm-specific artefacts. Luteolin interacts with Ser378 in CYP51 and Tyr84/Asp120 in SAP2, indicating dual-target engagement, whereas apigenin exhibits a similar cross-target binding pattern. Flavonoids are well documented to act on multiple fungal processes, including inhibition of efflux pumps, membrane permeabilisation, biofilm suppression, and direct protein interactions [1]. Previous work has demonstrated that flavones and flavonols, including apigenin derivatives, perturb fungal membranes, inhibit hyphal growth, and downregulate genes involved in virulence and biofilm formation, further supporting their multi-target potential [37]. The present *in silico* predictions and residue-level insights reinforce the notion that flavonoids act as diverse antifungal agents through multiple mechanisms. These secondary-lead multi-target inhibitors identified in this study may impose a greater evolutionary burden on *C. albicans*, as resistance would require concurrent adaptive mutations across multiple enzyme systems [37]. Collectively, these findings support the concept that the antifungal activity of plant phenolics arises from converging mechanisms rather than a single binary mode of action, providing a rationale for prioritising these flavonoids for further experimental validation.

SwissADME and pkCSM analyses corroborated the pharmacokinetic suitability of the primary and secondary prioritised compounds, consistent with their consensus-based selection. All primary and secondary prioritised lead compounds were predicted to be non-hepatotoxic, non-mutagenic, and non-BBB-permeant, suggesting favourable preliminary safety profiles. High human intestinal absorption (HIA) is essential for oral treatment of systemic candidiasis; apigenin and ellagic acid demonstrated particularly high HIA, comparable to or exceeding that of fluconazole. Apigenin exhibited the highest permeability across Caco-2 cells, suggesting efficient passive diffusion. In contrast, quercetin exhibited lower permeability, consistent with the literature indicating that flavonoid bioavailability is often limited by rapid Phase II metabolism [38], which may necessitate nanoformulations or liposomal

delivery for clinical translation. Notably, quercetin, luteolin, and apigenin interacted with CYP3A4 and CYP2D6, which could lead to metabolic interactions with commonly prescribed drugs, particularly in polypharmacy contexts [39,40]. By contrast, ellagic acid showed no inhibitory activity against the tested CYP isoforms, suggesting a favourable metabolic safety profile. Except for apigenin, all compounds triggered PAINS alerts, a common occurrence among polyphenolic natural products due to multiple hydroxyl groups [41]; however, observed hydrogen bonding, π - π stacking, and site-specific residue interactions suggest target-directed binding rather than nonspecific surface interference. Despite these favourable *in silico* predictions, experimental enzymatic assays remain essential to confirm antifungal efficacy and specificity.

Limitations of the study

Several limitations of this study should be explicitly acknowledged. Firstly, molecular docking is inherently static: it captures a single low-energy binding pose. Still, it cannot fully model the conformational flexibility of protein–ligand complexes over time, solvent-mediated thermodynamic effects, or induced-fit conformational changes that may alter binding geometry under physiological conditions. Accordingly, the binding affinities and consensus Z-scores reported here represent predictive prioritisation metrics rather than experimentally determined binding constants. Molecular dynamics (MD) simulations, preferably extending beyond 100 ns, constitute a necessary next step to evaluate complex stability, characterise conformational persistence, estimate binding free energies through MM-GBSA or MM-PBSA approaches, and determine whether the proposed interaction mechanisms particularly the SAP2 flap-locking effect of ellagic acid and the CYP51 substrate-channel blockade by quercetin, remain stable under dynamic conditions. Secondly, although SwissADME and pkCSM provide useful preliminary pharmacokinetic estimates, these platforms rely on descriptor-based predictive models and possess inherent limitations. Predicted HIA and Caco-2 permeability values do not account for active transport processes, efflux systems, metabolic instability, or microbiome-

mediated biotransformation. In addition, the PAINS alerts observed for quercetin, ellagic acid, and luteolin necessitate experimental counter-screening assays to exclude nonspecific reactivity or assay interference. Thirdly, no experimental cytotoxicity or selectivity data against mammalian host cells were generated in the present study. Therefore, selectivity indices and therapeutic windows remain unknown and must be established experimentally before any translational consideration. *In vitro* minimum inhibitory concentration (MIC) assays against both planktonic and biofilm forms of *C. albicans*, followed by *in vivo* validation in appropriate candidiasis models, are essential for determining whether the computational consensus prioritisation reported here translates into genuine antifungal efficacy. Until such validation studies are performed, the compounds identified in this work should be regarded strictly as computationally prioritised antifungal candidates.

Conclusions

This study used tri-engine consensus docking (AutoDock Vina, AutoDock4, LeDock) to evaluate *P. granatum* leaf phytochemicals as dual-target inhibitors of *Candida albicans* CYP51 and SAP2. Quercetin and ellagic acid emerged as primary lead target-specific specialists, with quercetin predicted to interact with the CYP51 substrate access channel through a mechanism potentially distinct from azole resistance pathways. In contrast, ellagic acid was predicted to restrict the mobility of the Tyr84 flap of SAP2, offering a structural basis for its reported anti-virulence effects—both hypotheses requiring MD simulation and experimental validation to confirm. Among the secondary comparative candidates, luteolin and apigenin acted as multi-target generalists, showing consistent binding across all platforms, suggesting a higher evolutionary barrier to resistance. ADMET profiling indicated favourable drug-likeness, pharmacokinetics, and toxicity for all leads. The consensus docking prioritisation and ADMET profiling present a coherent case for advancing quercetin and ellagic acid as primary leads, and luteolin and apigenin as secondary multi-target candidates into molecular dynamics simulation and experimental antifungal validation.

Disclosures

Acknowledgements

The author sincerely thanks Bilal Muazu Yunusa for generously providing access to his computer system, which was essential for performing the molecular docking simulations and all the visual analysis involved in this study.

Conflict of interest statement

The authors declare no conflict of interest.

Data availability statement

All software versions, parameters, input and output files are documented and can be shared upon reasonable request.

Funding statement

This study received no specific grant from any funding agency in the public, commercial, or not-for-profit organisations.

Author contributions

Shukurana Sulaiman Adam conceptualised and designed the study; performed molecular docking analyses, consensus scoring, visualisation, and ADMET profiling; interpreted the data; prepared the figures and tables; conducted the literature review; and wrote, revised, and approved the final manuscript.

Final approval statement

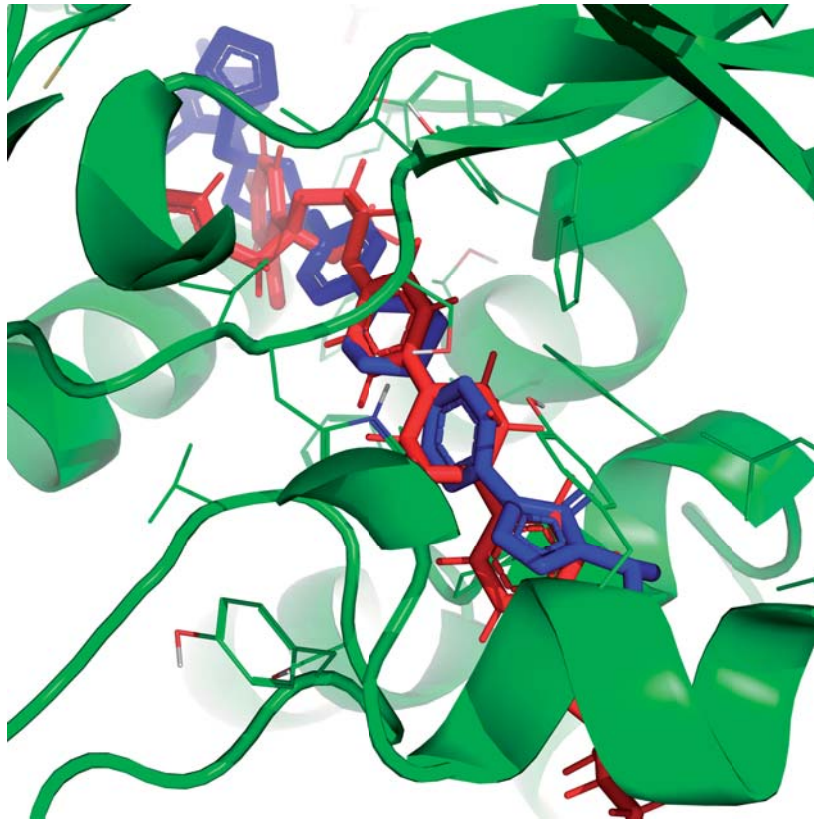
The author confirms approval of the final version of the manuscript and agrees to its submission for publication in the Journal of Medical Science.

References

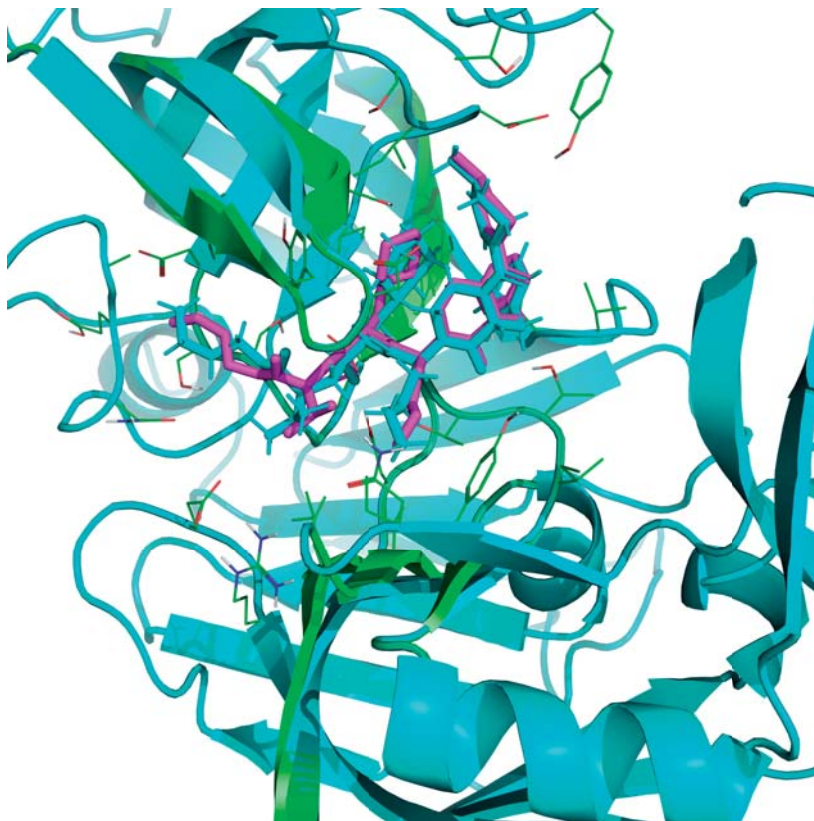
1. Al Aboody MS, Mickymaray S. Anti-Fungal Efficacy and Mechanisms of Flavonoids. *Antibiotics*. 2020 Jan 26;9(2):45. <https://doi.org/10.3390/antibiotics9020045>
2. Maphetu N, Unuofin JO, Masuku NP, Olisah C, Lebelo SL. Medicinal uses, pharmacological activities, phytochemistry, and the molecular mechanisms of *Punica granatum* L. (pomegranate) plant extracts: A review. *Biomed Pharmacother*. 2022 Sep;153:113256. <https://doi.org/10.1016/j.biopha.2022.113256>
3. Singh B, Singh JP, Kaur A, Singh N. Phenolic compounds as beneficial phytochemicals in pomegranate (*Punica granatum* L.) peel: A review. *Food Chem*. 2018 Sep;261:75–86. <https://doi.org/10.1016/j.foodchem.2018.04.039>
4. Brighenti V, Iseppi R, Pinzi L, Mincuzzi A, Ippolito A, Messi P, et al. Antifungal Activity and DNA Topoisomerase Inhibition of Hydrolysable Tannins from *Punica granatum* L. *Int J Mol Sci*. 2021 Apr 17;22(8):4175. <https://doi.org/10.3390/ijms22084175>
5. Trabelsi A, El Kaibi MA, Abbassi A, Horchani A, Chekir-Ghedira L, Ghedira K. Phytochemical Study and Antibacterial and Antibiotic Modulation Activity of *Punica granatum* (Pomegranate) Leaves. *Scientifica*. 2020 Mar 31;2020:1–7. <https://doi.org/10.1155/2020/8271203>
6. Yisimayili Z, Chao Z. A review on phytochemicals, metabolic profiles and pharmacokinetics studies of the different parts (juice, seeds, peel, flowers, leaves and bark) of pomegranate (*Punica granatum* L.). *Food Chem*. 2022 Nov;395:133600. <https://doi.org/10.1016/j.foodchem.2022.133600>
7. Yu M, Gouvinhas I, Chen J, Zhu Y, Deng J, Xiang Z, et al. Unlocking the therapeutic treasure of pomegranate leaf: A comprehensive review on phytochemical compounds, health benefits, and future prospects. *Food Chem X*. 2024 Oct;23:101587. <https://doi.org/10.1016/j.fochx.2024.101587>
8. Nawwar MAM, Hussein SAM, Merfort I. Leaf phenolics of *Punica granatum*. *Phytochemistry*. 1994 Nov;37(4):1175–7. [https://doi.org/10.1016/S0031-9422\(00\)89552-7](https://doi.org/10.1016/S0031-9422(00)89552-7)
9. Xiang L, Xing D, Lei F, Wang W, Xu L, Nie L, et al. Effects of season, variety, and processing method on ellagic acid content in pomegranate leaves. *Tsinghua Sci Technol*. 2008 Aug;13(4):460–5. [https://doi.org/10.1016/S1007-0214\(08\)70074-9](https://doi.org/10.1016/S1007-0214(08)70074-9)
10. Thukral S, Sharma A, Jyoti A, Gunjal M, Rasane P, Kaur S, et al. A literature review of pomegranate leaf: Extraction techniques, phytochemistry, and health implications. *South Afr J Bot*. 2025 Dec;187:632–44. <https://doi.org/10.1016/j.sajb.2025.10.038>
11. Mestry SN, Gawali NB, Gursahani MS, Pai SA, Dhodi JB, Juvekar AR. Inhibition of advanced glycation end products by *Punica granatum* Linn. leaves and its antioxidant activity. *Orient Pharm Exp Med*. 2018 Jun;18(2):97–105. <https://doi.org/10.1007/s13596-018-0309-y>
12. Lionta E, Spyrou G, Vassilatis D, Cournia Z. Structure-Based Virtual Screening for Drug Discovery: Principles, Applications and Recent Advances. *Curr Top Med Chem*. 2014 Oct 15;14(16):1923–38. <https://doi.org/10.2174/1568026614666140929124445>
13. Valdés-Tresanco MS, Valdés-Tresanco ME, Valiente PA, Moreno E. AMDock: a versatile graphical tool for assisting molecular docking with Autodock Vina and Autodock4. *Biol Direct*. 2020 Dec;15(1):12. <https://doi.org/10.1186/s13062-020-00267-2>
14. Goodsell DS, Sanner MF, Olson AJ, Forli S. The AutoDock suite at 30. *Protein Sci*. 2021 Jan;30(1):31–43. <https://doi.org/10.1002/pro.3934>
15. Eghbali S, Askari SF, Avan R, Sahebkar A. Therapeutic Effects of *Punica granatum* (Pomegranate): An Updated Review of Clinical Trials. Gumpricht E, editor. *J Nutr Metab*. 2021 Nov 16;2021:1–22. <https://doi.org/10.1155/2021/5297162>
16. Wang D, Özen C, Abu-Reidah IM, Chigurupati S, Patra JK, Horbanczuk JO, et al. Vasculoprotective Effects of Pomegranate (*Punica granatum* L.). *Front Pharmacol*. 2018 May 24;9:544. <https://doi.org/10.3389/fphar.2018.00544>
17. Read E, Deseo MA, Hawes M, Rochfort S. Identification of potentially cytotoxic phenolics present in pomegranates (*Punica granatum* L.). *Anim Feed Sci Technol*. 2019 May;251:187–97. <https://doi.org/10.1016/j.anifeedsci.2019.03.012>
18. Foglietta F, Querio G, Sanna C, Canaparo R, Marenngo A, Serpe L, et al. Comparative antioxidant activity

- of pomegranate leaf extract and derived metabolites in single and co-cultured cell lines. *Sci Rep*. 2025 Oct 16;15(1):36266. <https://doi.org/10.1038/s41598-025-20130-6>
19. O'Boyle NM, Banck M, James CA, Morley C, Vandermeersch T, Hutchison GR. Open Babel: An open chemical toolbox. *J Cheminformatics*. 2011 Dec;3(1):33. <https://doi.org/10.1186/1758-2946-3-33>
 20. Hanwell MD, Curtis DE, Lonie DC, Vandermeersch T, Zurek E, Hutchison GR. Avogadro: an advanced semantic chemical editor, visualization, and analysis platform. *J Cheminformatics*. 2012 Dec;4(1):17. <https://doi.org/10.1186/1758-2946-4-17>
 21. Velázquez-Libera JL, Durán-Verdugo F, Valdés-Jiménez A, Núñez-Vivanco G, Caballero J. LigRMSD: a web server for automatic structure matching and RMSD calculations among identical and similar compounds in protein-ligand docking. Ponty Y, editor. *Bioinformatics*. 2020 May 1;36(9):2912–4. <https://doi.org/10.1093/bioinformatics/btaa018>
 22. Liu N, Xu Z. Using LeDock as a docking tool for computational drug design. *IOP Conf Ser Earth Environ Sci*. 2019 Feb 23;218:012143. <https://doi.org/10.1088/1755-1315/218/1/012143>
 23. BIOVIA. Discovery Studio Visualizer (Internet). San Diego, CA: Dassault Systèmes; 2025. Available from: 3ds.com
 24. Daina A, Michielin O, Zoete V. SwissADME: a free web tool to evaluate pharmacokinetics, drug-likeness and medicinal chemistry friendliness of small molecules. *Sci Rep*. 2017 Mar 3;7(1):42717. <https://doi.org/10.1038/srep42717>
 25. Pires DEV, Blundell TL, Ascher DB. pkCSM: Predicting Small-Molecule Pharmacokinetic and Toxicity Properties Using Graph-Based Signatures. *J Med Chem*. 2015 May 14;58(9):4066–72. <https://doi.org/10.1021/acs.jmedchem.5b00104>
 26. Whaley SG, Berkow EL, Rybak JM, Nishimoto AT, Barker KS, Rogers PD. Azole Antifungal Resistance in *Candida albicans* and Emerging Non-*albicans Candida* Species. *Front Microbiol*. 2017 Jan 12;7. <https://doi.org/10.3389/fmicb.2016.02173>
 27. McCombs NL, Moreno-Chicano T, Carey LM, Franzen S, Hough MA, Ghiladi RA. Interaction of Azole-Based Environmental Pollutants with the Coelomic Hemoglobin from *Amphitrite ornata*: A Molecular Basis for Toxicity. *Biochemistry*. 2017 May 2;56(17):2294–303. <https://doi.org/10.1021/acs.biochem.7b00041>
 28. Tan Y, Lin Q, Yao J, Zhang G, Peng X, Tian J. In vitro outcomes of quercetin on *Candida albicans* planktonic and biofilm cells and in vivo effects on vulvovaginal candidiasis. Evidences of its mechanisms of action. *Phytomedicine*. 2023 Jun;114:154800. <https://doi.org/10.1016/j.phymed.2023.154800>
 29. Gao M, Wang H, Zhu L. Quercetin Assists Fluconazole to Inhibit Biofilm Formations of Fluconazole-Resistant *Candida Albicans* in In Vitro and In Vivo Antifungal Managements of Vulvovaginal Candidiasis. *Cell Physiol Biochem*. 2016;40(3–4):727–42. <https://doi.org/10.1159/000453134>
 30. Lee JH, Kim YG, Park I, Lee J. Antifungal and antibiofilm activities of flavonoids against *Candida albicans*: Focus on 3,2'-dihydroxyflavone as a potential therapeutic agent. *Biofilm*. 2024 Dec;8:100218. <https://doi.org/10.1016/j.biofilm.2024.100218>
 31. Borelli C, Ruge E, Lee JH, Schaller M, Vogelsang A, Monod M, et al. X-ray structures of Sap1 and Sap5: Structural comparison of the secreted aspartic proteinases from *Candida albicans*. *Proteins Struct Funct Bioinforma*. 2008 Sep;72(4):1308–19. <https://doi.org/10.1002/prot.22021>
 32. Bhakat S, Söderhjelm P. Flap Dynamics in Pepsin-Like Aspartic Proteases: A Computational Perspective Using Plasmepsin-II and BACE-1 as Model Systems. *J Chem Inf Model*. 2022 Feb 28;62(4):914–26. <https://doi.org/10.1021/acs.jcim.1c00840>
 33. Mahanti M, Bhakat S, Nilsson UJ, Söderhjelm P. Flap Dynamics in Aspartic Proteases: A Computational Perspective. *Chem Biol Drug Des*. 2016 Aug;88(2):159–77. <https://doi.org/10.1111/cbdd.12745>
 34. Nejatbakhsh S, Ilkhanizadeh-Qomi M, Razzaghi-Abayaneh M. The Effects of Ellagic Acid on Growth and Biofilm Formation of *Candida albicans*. *J Med Microbiol Infect Dis*. 2020 Jan 1;8(1):14–8. <https://doi.org/10.29252/JoMMID.8.1.14>
 35. Li Z, Guo X, Dawuti G, Aibai S. Antifungal Activity of Ellagic Acid In Vitro and In Vivo. *Phytother Res*. 2015 Jul;29(7):1019–25. <https://doi.org/10.1002/ptr.5340>
 36. Mendes AGG, Campos CDL, Pereira-Filho JL, Pereira APA, Reis GSA, Araújo ÁWDMS, et al. Ellagic Acid Potentiates the Inhibitory Effects of Fluconazole Against *Candida albicans*. *Antibiotics*. 2024 Dec 4;13(12):1174. <https://doi.org/10.3390/antibiotics13121174>
 37. Ivanov M, Kannan A, Stojković DS, Glamočlija J, Calhelha RC, Ferreira ICFR, et al. Flavones, Flavonols, and Glycosylated Derivatives—Impact on *Candida albicans* Growth and Virulence, Expression of CDR1 and ERG11, Cytotoxicity. *Pharmaceuticals*. 2020 Dec 30;14(1):27. <https://doi.org/10.3390/ph14010027>
 38. Otto DP, Otto A, De Villiers MM. Experimental and mesoscale computational dynamics studies of the relationship between solubility and release of quercetin from PEG solid dispersions. *Int J Pharm*. 2013 Nov;456(2):282–92. <https://doi.org/10.1016/j.ijpharm.2013.08.039>
 39. Vander Schaaf M, Luth K, Townsend DM, Chessman KH, Mills CM, Garner SS, et al. CYP3A4 drug metabolism considerations in pediatric pharmacotherapy. *Med Chem Res*. 2024 Dec;33(12):2221–35. <https://doi.org/10.1007/s00044-024-03360-7>
 40. Nahid NA, Johnson JA. CYP2D6 pharmacogenetics and phenoconversion in personalized medicine. *Expert Opin Drug Metab Toxicol*. 2022 Nov 2;18(11):769–85. <https://doi.org/10.1080/17425255.2022.2160317>
 41. Baell J, Walters MA. Chemistry: Chemical con artists foil drug discovery. *Nature*. 2014 Sep 25;513(7519):481–3. <https://doi.org/10.1038/513481a>

Supplementary files



Supplementary file 1.



Supplementary file 2.